Carbohydrate Polymers **5** (1985) 407–422

Optical Rotation Behavior of Xanthan in Mixtures of Water and Cadoxen

Hiroko Kitagawa, Takahiro Sato, Takashi Norisuye and Hiroshi Fujita

Department of Macromolecular Science, Osaka University, Toyonaka, Osaka 560, Japan

(Received: 21 April 1985)

SUMMARY

Optical rotatory dispersion (ORD) data were obtained for a sample of the sodium salt of xanthan gum dissolved in water–cadoxen mixtures at 25°C. The double-helical dimer of the polysaccharide was previously found to dissociate directly to single chains when w_{cad} (the weight fraction of cadoxen in the mixed solvent) increases from 0·3 to 0·8. ORD data were also obtained for solutions prepared by diluting xathan solutions at low concentration in cadoxen with water to different w_{cad} values. From previous work these were taken as those for single dissociated chains in the mixed solvent. These sets of data led to the finding that the specific rotation at 300 nm wavelength does not reflect the dissociation of the xanthan double helix in water–cadoxen mixtures, but the Moffitt parameter does. This parameter gave evidence that single coiling chains in cadoxen become intramolecularly ordered to a conformation similar to that of the individual chains in the double helix when the solution is diluted with water to w_{cad} below 0·4.

INTRODUCTION

Recently, the authors demonstrated by light scattering, viscosity and sedimentation measurements (Sato *et al.*, 1984*a*,*b*,*c*) that xanthan (sodium salt) dissolves as rod-like dimers having a double-stranded helical structure in 0·1 M aqueous NaCl and as single random coils in tris(ethylenediamine) cadmium dihydroxide (cadoxen). The authors

Carbohydrate Polymers 0144-8617/85/$03.30 –

also derived the following conclusions from a similar study (Sato *et al.*, 1985) on this polysaccharide dissolved in water–cadoxen mixtures: (1) with increasing w_{cad} (the weight fraction of cadoxen in the mixed solvent), the double helix of xanthan progressively dissociates to single chains without going through a partial melting stage. Thus, the solution with a given w_{cad} comprises two solute species: double helix and single chain; (2) the single chains assume more extended conformations than the random coil in pure cadoxen as w_{cad} departs from unity.

In this work, optical rotation measurements were made on the sodium salt of xanthan in water–cadoxen mixtures to examine the dissociation of the xanthan double helix and the conformation of single dissociated chains from a different angle, i.e. by looking at the local properties of the polysaccharide.

EXPERIMENTAL

The previously investigated sample X9-3 (Sato *et al.*, 1985) was used. Its weight-average molecular weight M_w was $9{\cdot}94 \times 10^5$ in 0·1 M aqueous NaCl and $4{\cdot}93 \times 10^5$ in cadoxen; note that the ratio of these M_w values is almost equal to 2.

Two methods were used to make up test solutions: in one, the sample was directly dissolved in water–cadoxen mixtures of the desired w_{cad} at different polymer concentrations c, and in the other the sample was first dissolved in pure cadoxen at different c and then each solution was diluted with water to the desired w_{cad}. In the following, the solutions prepared by the former method are referred to as cadoxen-mixed water (CMW) solutions, and those by the latter method as water-diluted cadoxen (WDC) solutions. This distinction is important because, according to the authors' previous investigation (Sato *et al.*, 1985), these solutions contain different kinds of polymer species, i.e. double helices and single chains in CMW solutions, and single chains and their aggregates in WDC solutions.

Optical rotatory dispersion (ORD) curves were recorded at 25°C on a JASCO ORD/UV-5 spectropolarimeter with 10-cm cylindrical quartz cells, 5–10 h after the preparation of solutions. No variation in optical rotation with time was observed for any of the solutions studied. This is consistent with our previous finding from light scattering and viscometry

(Sato *et al.*, 1984*b*, 1985) that, up to 24 h after the preparation of solutions, no appreciable degradation of the sodium salt of xanthan gum occurs in water–cadoxen mixtures. The specific rotation $[\alpha]_\lambda$ at wavelength λ was evaluated from $[\alpha]_\lambda = \alpha_\lambda/(cL)$, where α_λ is the optical rotation at λ and L, the cell length (in cm). In the range of c examined ($\lesssim 0{\cdot}75 \times 10^{-2}$ g cm^{-3}), $[\alpha]_\lambda$ for CMW solutions were independent of c, while those for WDC solutions increased very slightly with decreasing c for w_{cad} between 0·5 and 0·7, and were extrapolated to $c = 0$.

In previous work (Sato *et al.*, 1985), we showed that no aggregates are formed in WDC solutions of vanishingly low polymer concentrations, and took advantage of this fact to determine $\langle S^2 \rangle_z$ (the mean-square radius of gyration) and $[\eta]$ (the intrinsic viscosity) of a single xanthan chain in CMW of a given w_{cad}. Anticipating that this method should be valid for $[\alpha]_\lambda$ as well, we have taken infinite-dilution values of $[\alpha]_\lambda$ in WDC as giving $[\alpha]_\lambda$ of a single xanthan chain in CMW of any composition.

RESULTS AND DISCUSSION

Specific rotation

Figure 1 illustrates ORD curves for CMW solutions with $c = 0{\cdot}50 \times 10^{-2}$ g cm^{-3}. All these curves decline monotonically with decreasing wavelength.

The unfilled circles in Fig. 2 show $[\alpha]_{300}$ at 300 nm for CMW solutions as a function of w_{cad}. With increasing w_{cad}, $[\alpha]_{300}$ increases gradually to a maximum at a w_{cad} of 0·65 and then decreases sharply to the value in pure cadoxen for higher w_{cad}. The latter range of w_{cad} does not conform to the range $0{\cdot}3 \lesssim w_{cad} \lesssim 0{\cdot}8$ in which M_w, $\langle S^2 \rangle_z^{1/2}$ and $[\eta]$ were found to decrease (Sato *et al.*, 1985). Further, the w_{cad} dependence of M_w, $\langle S^2 \rangle_z^{1/2}$ and $[\eta]$ exhibited no maximum in contrast to the w_{cad} dependence of $[\alpha]_{300}$.

The infinite-dilution values of $[\alpha]_{300}$ for WDC solutions are shown by filled circles in Fig. 2. They almost follow the curve fitting the unfilled circles, suggesting that the change in the sodium salt of xanthan gum with w_{cad} is essentially reversible. However, this cannot be correct since, as mentioned in the Experimental section, different kinds of polymer species are present in CMW and WDC solutions.

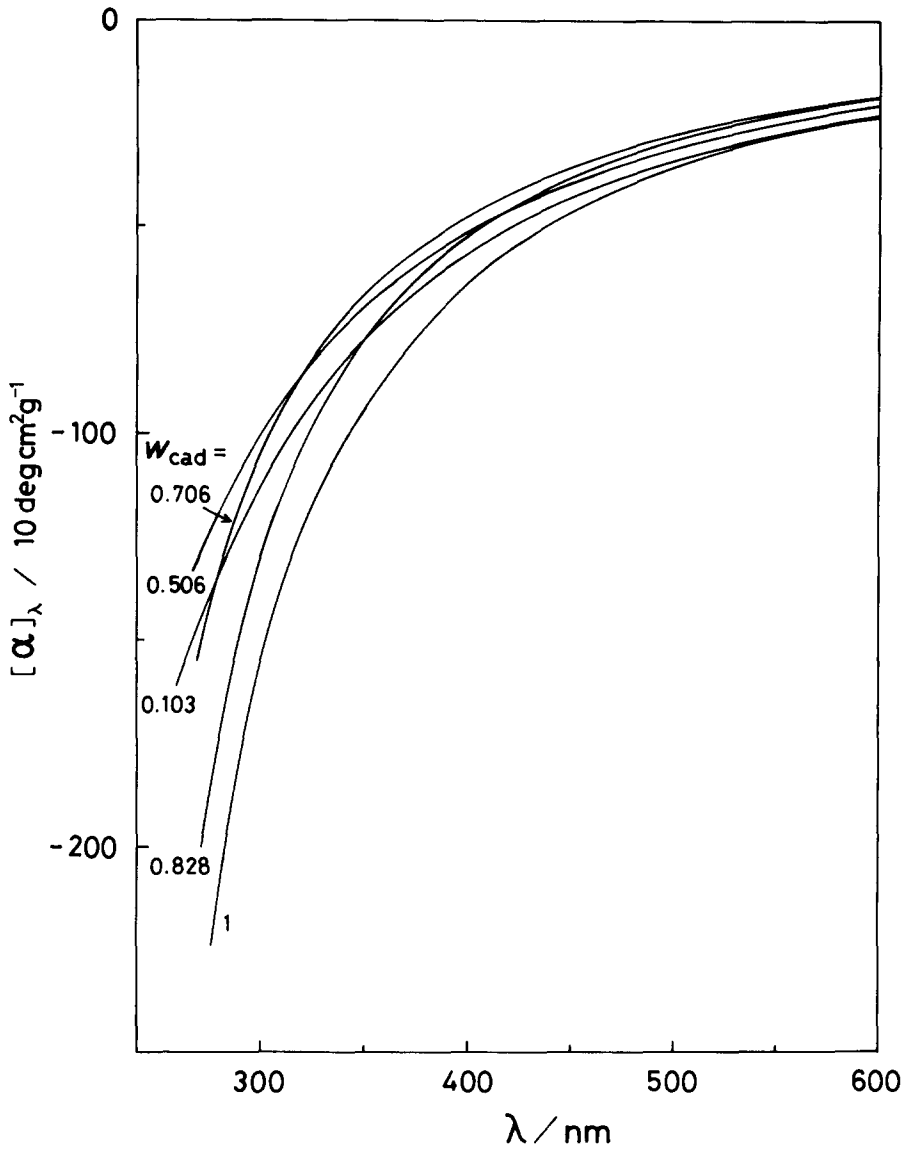

Fig. 1. ORD curves for the sodium salt of xanthan gum (sample X9-3) in CMW at different w_{cad}: temperature 25°C.

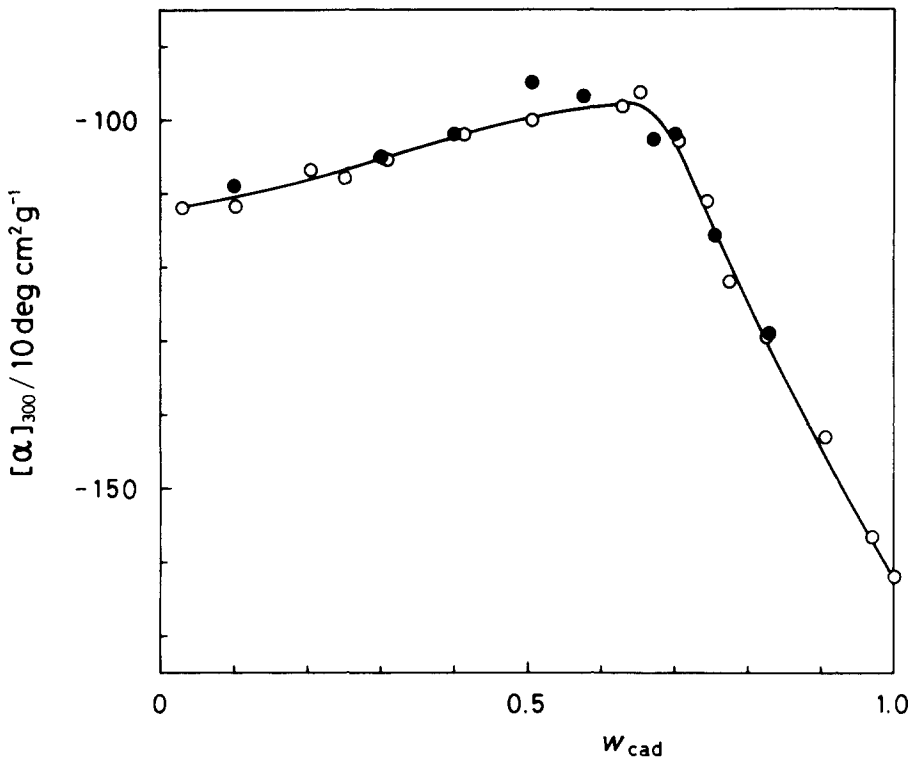

Fig. 2. Dependence of $[\alpha]_{300}$ on w_{cad} for CMW (○) and WDC (●) solutions at 25°C.

According to the previous finding mentioned in the Introduction, we can express $[\alpha]_{300}$ for the sodium salt of xanthan in a CMW solution as

$$[\alpha]_{300} = f[\alpha]^{D}_{300} + (1-f)[\alpha]^{S}_{300} \quad (1)$$

where the superscripts D and S refer to the double helix and single chain species, respectively, and f is the weight fraction of the former. For the reason mentioned in the Experimental section, we substitute the values of $[\alpha]_{300}$ given by the filled circles in Fig. 2 for $[\alpha]^{S}_{300}$ in eqn (1). These values essentially agree with those of $[\alpha]_{300}$ over the entire range of w_{cad}, as can be seen from Fig. 2. Hence, it follows from eqn (1) that

$$f([\alpha]^{D}_{300} - [\alpha]^{S}_{300}) \simeq 0$$

which gives $f \simeq 0$ for any w_{cad} if $[\alpha]^{D}_{300} \neq [\alpha]^{S}_{300}$. This contradicts our previous finding (Sato *et al.*, 1985) from light scattering and viscosity data that f decreases from unity to zero with increasing w_{cad} from 0·3 to 0·8. Thus, we must conclude that at least for $w_{cad} \lesssim 0{\cdot}8$

$$[\alpha]^{D}_{300} \simeq [\alpha]^{S}_{300} \tag{2}$$

This result looks odd, since it would be natural to expect that, because of their distinct difference in conformation, the double helix and single chain species should have different specific rotations. A possible explanation is that $[\alpha]_{300}$ values for these two species happen to coincide as a result of unexpected solvent effects. At any rate, the composition dependence of $[\alpha]_{300}$ for CMW solutions in Fig. 2 can give little information about the dissociation of the double helix to single chains.

Moffitt parameter

The Moffitt parameter b_0 is defined by (Moffitt & Yang, 1956)

$$[m']_{\lambda} = \frac{a_0 \lambda_0^2}{\lambda^2 - \lambda_0^2} + \frac{b_0 \lambda_0^4}{(\lambda^2 - \lambda_0^2)^2} \tag{3}$$

where a_0 and λ_0 are constants and $[m']_{\lambda}$, the mean residue rotation is defined by

$$[m']_{\lambda} = \frac{3}{n_{\lambda}^2 + 2} M_0 [\alpha]_{\lambda} \tag{4}$$

n_{λ} and M_0 are the solvent refractive index at wavelength λ and the molar mass of a residue, respectively. Equation (3) is often used for analysing ORD data for α-helical polypeptides (Urnes & Doty, 1961; Teramoto & Fujita, 1976); it is well known that b_0 is usually less affected by solvent conditions than $[\alpha]_{\lambda}$. Because of this property of the Moffitt parameter it is useful for investigating the change in the conformation of a polypeptide in a mixed solvent of varying composition.

The circular dichroism data on xanthan reported by Morris *et al.* (1977) show absorption peaks at about 205 and 220 nm. Milas & Rinaudo (1979) found essentially the same peak absorption wavelengths for the sodium salt of xanthan. These wavelengths are close to those observed for α-helical polypeptides (Urnes & Doty, 1961).

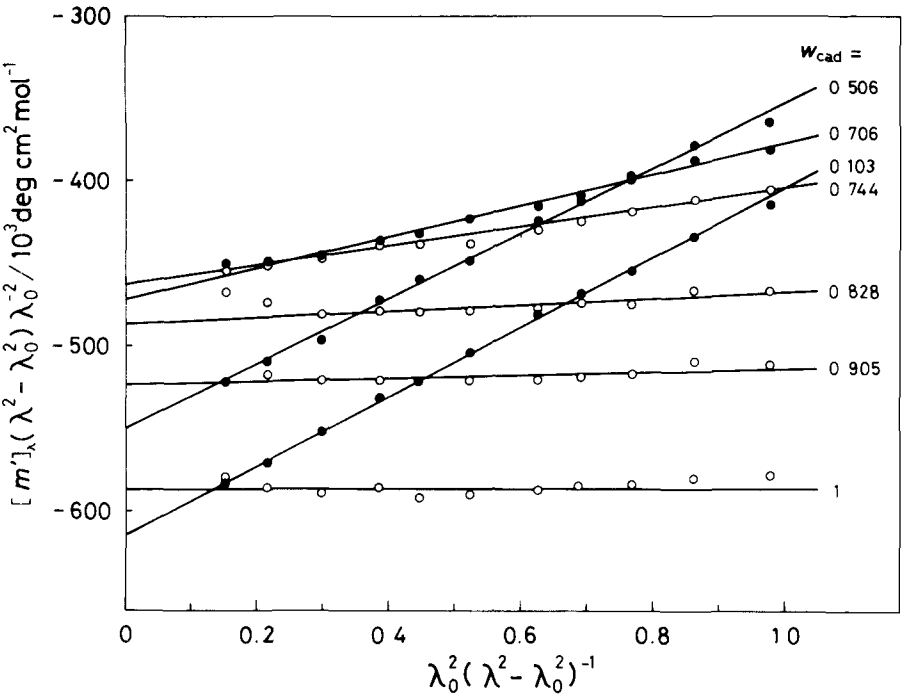

Fig. 3. Moffitt plots of ORD data for CMW solutions.

In view of this similarity, we decided to test the applicability of eqn (3) to our xanthan data for λ between 600 and 300 nm, which is the range usually used for polypeptide conformation determination. For this purpose λ_0 in eqn (3) was estimated to be 211 nm from the ORD data in pure cadoxen, and b_0 in this solvent was assumed to be zero; M_0 for our xanthan sample is 460 g mol^{-1} (Sato *et al.*, 1984*a*). Interestingly, the λ_0 value for xanthan is very close to the optimum λ_0 of 212 nm for polypeptides (Urnes & Doty, 1961).

Figure 3 shows the Moffitt plots constructed from our data for CMW solutions. The plotted points for each w_{cad} follow a straight line, demonstrating the applicability of eqn (3) to the ORD data for xanthan in water-cadoxen mixtures (see also the Appendix). The values of b_0 determined from the straight lines are shown as a function of w_{cad} in Fig. 4, where the previously determined w_{cad} dependence of M_w, $\langle S^2\rangle_z^{1/2}$ and $[\eta]$ (Sato *et al.*, 1985) is included for comparison. It can

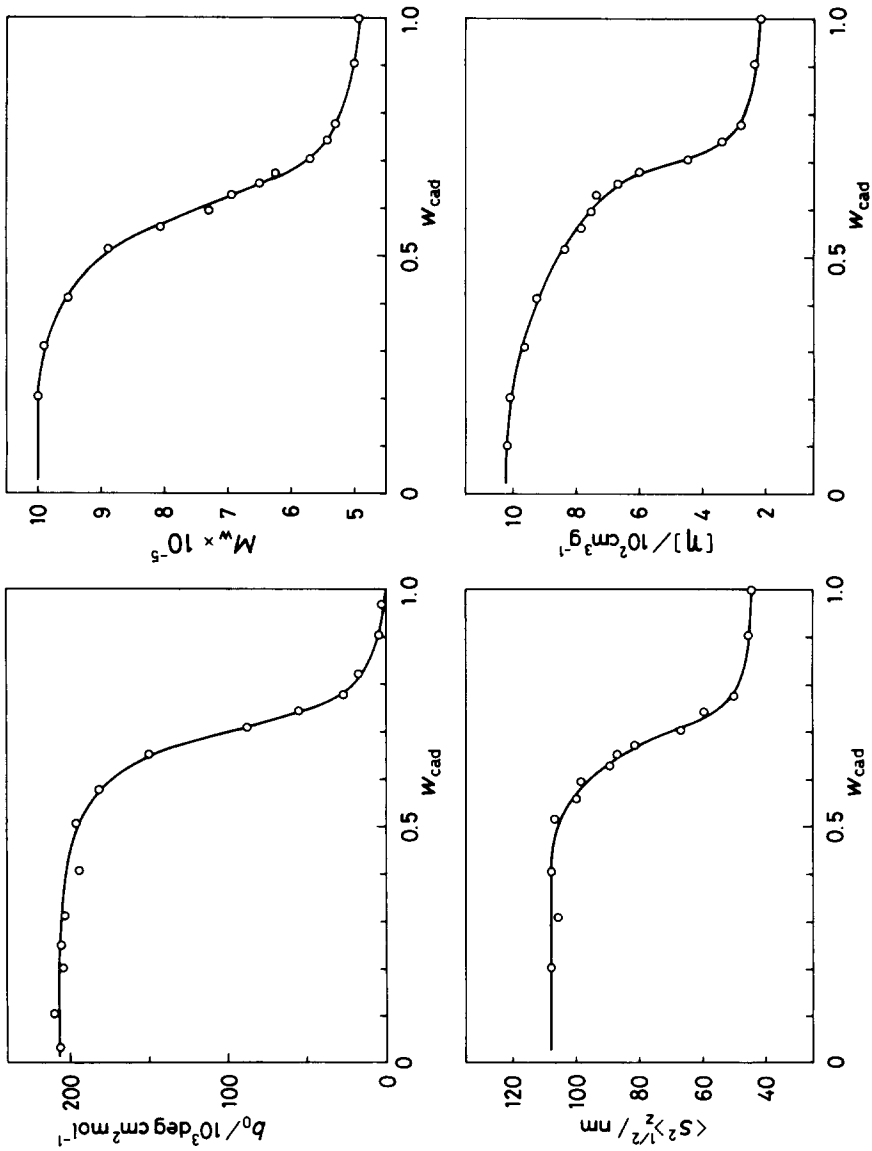

Fig. 4. Composition dependence of b_0, M_w, $\langle S^2 \rangle_z^{1/2}$ and $[\eta]$ for sample X9-3 in CMW at 25°C.

be seen that b_0 stays essentially constant up to $w_{cad} \sim 0{\cdot}3$ and decreases fairly sharply to about zero with increasing w_{cad} to 0·8. This behaviour is very similar to that of the other physical quantities shown in Fig. 4. In contrast to $[\alpha]_{300}$, b_0 exhibits no maximum at any w_{cad}.

It was found that the ORD data obtained for WDC solutions can also be fitted by eqn (3). The b_0 values were slightly dependent on c (see the Experimental section) and extrapolated to infinite dilution. The results are shown in Fig. 5(a), where the dashed line taken from Fig. 4 illustrates the w_{cad} dependence of b_0 in CMW.

Like $[\alpha]_{300}$, b_0 in CMW can be expressed by

$$b_0 = f b_0^D + (1 - f)\, b_0^S \tag{5}$$

where b_0^D and b_0^S denote the b_0 values associated, respectively, with the double helix and single chain species at the appropriate w_{cad}. The b_0 values represented by the open circles in Fig. 5 are taken as b_0^S. The f values for w_{cad} at these circles can be computed from the M_w versus w_{cad} curve in Fig. 4 (note that f is given by $(M_w - M_w^S)/(M_w^D - M_w^S)$ where M_w^D and M_w^S are the molecular weights of the double helix and single chain species, respectively). Thus, with the dashed curve for b_0 in Fig. 5, it is possible to estimate b_0^D as a function of w_{cad} from eqn (5). The results, which are shown in Fig. 5(b), indicate that b_0^D is essentially independent of w_{cad} in the range shown; note that b_0^D at higher w_{cad} values are less accurate, since f in this composition range is very small.

The problem lies in how to interpret these findings on b_0^D and b_0^S. If, as may be expected from previous studies on polypeptides in mixed solvents, b_0 for xanthan in water–cadoxen mixtures is not influenced by solvent effects, these parameters should depend on the intrinsic local chain conformations in the double helix and single chain species of the polysaccharide.

Our light scattering and viscosity data (Sato *et al.*, 1985) have shown that the structure of the double helix species in aqueous solution is either maintained intact or completely destroyed when cadoxen is added to the solvent. Thus, b_0^D should be independent of w_{cad} if it indeed reflects the chain conformation in the double helix. The b_0^D data in Fig. 5(b) behave in this way, at least for w_{cad} between 0·1 and 0·8. Hence, we can conclude that b_0^D in this w_{cad} range reflects only the contribution from the double-helical conformation of xanthan in CMW; in other words, it is essentially free from solvent effects. To be con-

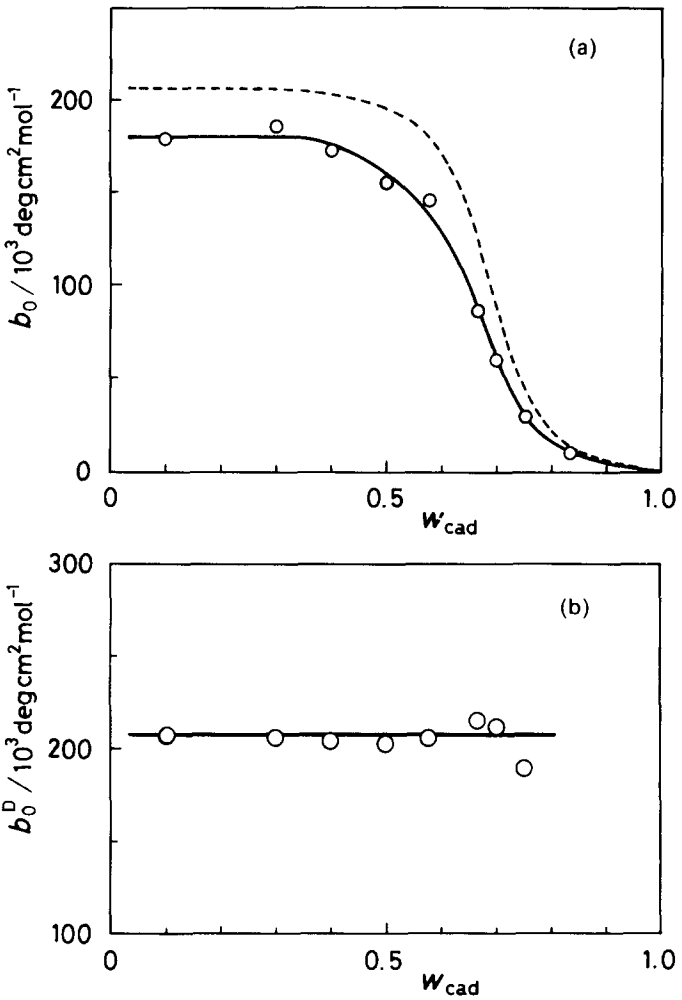

Fig. 5. (a) Composition dependence of b_0 for WDC solutions: – – –, b_0 for CMW solutions in Fig. 4; (b) values of b_0^D calculated from eqn (5) with the b_0 data in (a) and the M_w data in Fig. 4.

sistent with this conclusion, it seems reasonable to argue that b_0^S in the same composition range is also free from solvent effects and reflects the random coil conformation of the single chain species of the polysaccharide. If this is accepted, the significant variation in b_0^S with w_{cad}

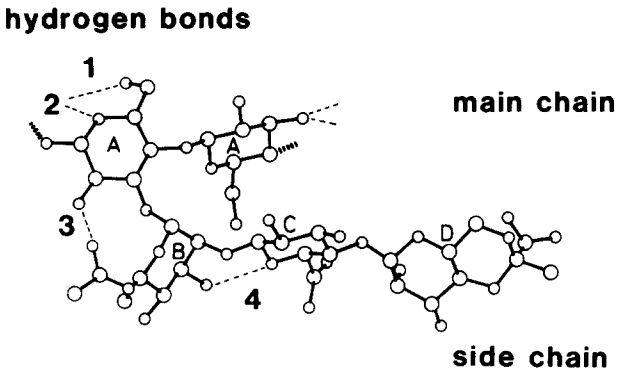

Fig. 6. Intramolecular hydrogen bonds per repeating unit in the double helix of xanthan (Okuyama *et al.*, 1980): A, β-D-glucose; B, 6-O-(acetyl)-α-D-mannose; C, β-D-glucuronate; D, 4,6-O-(1-carboxyethyl)-β-D-mannose.

as shown in Fig. 5(a) must be taken as a manifestation of the change in the local conformation of the randomly coiled chain.

Ordered conformation of single chains

The double-stranded helix of xanthan in the crystalline state has four intramolecular hydrogen bonds per repeating unit (Okuyama *et al.*, 1980), which are schematically shown by dashed lines in Fig. 6. These hydrogen bonds sustain the helical conformation of each xanthan chain, with the double-stranded structure stabilized by intermolecular hydrogen bonds. In previous work (Sato *et al.*, 1985), we observed that the dimensions of single xanthan chains in WDC solutions expand with a decrease in w_{cad}, and explained it as follows.

The sodium salt of xanthan gum in CMW maintains the double-helical structure at w_{cad} below 0·25. This implies that its intramolecular and intermolecular hydrogen bonds remain intact in this composition range. As cadoxen is added to increase w_{cad} above 0·3, these hydrogen bonds are successively broken and eventually they all disappear at $w_{cad} = 1$, i.e. in pure cadoxen, in which the polysaccharide assumes a random coil conformation. On the other hand, when w_{cad} is lowered below 0·8 by adding water to a cadoxen solution of a vanishingly low xanthan concentration, only the intramolecular hydrogen bonds are re-formed.

The bonds re-formed between adjacent main-chain glucoses (i.e. hydrogen bonds 1 and 2 in Fig. 6) almost completely hinder the internal rotation about the glucosidic oxygens, leading to an increase in chain dimensions. As w_{cad} is further lowered, more intramolecular hydrogen bonds are re-formed and more glucosidic linkages are fixed. Thus, the chain continues to expand with a decrease in w_{cad} until all the intramolecular hydrogen bonds are re-formed. This final stage was inferred from $[\eta]$ data to occur at $w_{cad} \sim 0{\cdot}6$.*

Reformation of intramolecular hydrogen bonds 3 and 4 in Fig. 6 causes the trisaccharide side chains of xanthan to align with the main chain. This should lead to a change in optical rotation, since the optical rotatory power of xanthan arises substantially from the chromophores of the O-acetate and carboxylate groups in the side chains (Morris *et al.*, 1977). Figure 6 indicates that cellobiose units with the four reformed hydrogen bonds 1, 2, 3 and 4 are forced to take a conformation similar to that of the units in the double helix. Thus, the optical rotation change induced by the side chain alignment must result in an increase in b_0^S with a decrease in w_{cad}. This increase in b_0^S should level off when intramolecular hydrogen bonding is completed. These considerations explain the increase and subsequent levelling-off of b_0^S with decreasing w_{cad} observed in Fig. 5(a).

The b_0^S data in Fig. 5(a) suggest that the completion of intramolecular hydrogen bonding occurs at a w_{cad} of about 0·4, which does not greatly differ from 0·6 estimated from $[\eta]$ data. The b_0^S values for $w_{cad} < 0{\cdot}4$ are fairly close to that for the intact double helix in CMW. This suggests that the single xanthan chain extended by intramolecular hydrogen bonds 1, 2, 3 and 4 should assume an ordered conformation similar to that of the individual chains in the double helix. In other words, the single xanthan coil in pure cadoxen is considered to become intramolecularly ordered when the solution is diluted with water to w_{cad} below 0·4. This may be compared with the conclusion of Norton *et al.* (1980, 1984) from stopped-flow polarimetric measurements that disordered xanthan chains in pure water at elevated temperature

* To be consistent with this value, the intramolecular hydrogen bonds in single chains dissociated from double helices in CMW below $w_{cad} \sim 0{\cdot}6$ must either remain intact or immediately be re-formed once broken in the dissociation of double helices. Thus, in water–cadoxen mixtures, the intramolecular hydrogen bonds are thermodynamically stabler than the intermolecular hydrogen bonds.

become intramolecularly ordered when potassium chloride is added to the solution.

APPENDIX

Many previous investigators (Holzwarth, 1976; Morris *et al.*, 1977; Milas & Rinaudo, 1979, 1981; Norton *et al.*, 1980, 1984; Rees, 1981; Frangou *et al.*, 1982) found that $[\alpha]_\lambda$ (λ = 260–365 nm) of xanthan in aqueous solutions of low ionic strength *increases* sigmoidally with increasing temperature. Rees, Holzwarth and Morris *et al.* ascribed this phenomenon to a thermally induced order-disorder conformation change of the polysaccharide. Probably, the ordered conformation at low temperature is the same double helix that the authors found in 0·1 M aqueous NaCl, since $[\alpha]_\lambda$ versus temperature curves for different NaCl concentrations almost merge with the curve for 0·1 M NaCl at low temperature (Holzwarth, 1976; Milas & Rinaudo, 1979, 1981). On the other hand, it is generally argued that disordered xanthan chains at high temperature are coils expanded by electrostatic repulsion of charged trisaccharide side chains.

Our study has shown that $[\alpha]_{300}$ in CMW sharply *decreases* with increasing w_{cad} from 0·65 to unity. This behaviour does not conform to what we might expect from the temperature dependence of $[\alpha]_\lambda$ in aqueous salt solutions, since increasing w_{cad} and temperature should disrupt the double-helical structure of xanthan. Our additional data for sample X9-3 in 0·01 M aqueous NaCl at different temperatures show that b_0 does not exhibit such incompatible behaviour.

Figure 7 shows that eqn (3) with $\lambda_0 = 211$ nm is also applicable to 0·01 M aqueous NaCl solutions of the sodium salt of xanthan gum. The temperature dependence of $[\alpha]_{300}$ and b_0 is illustrated in Fig. 8. With an increase in temperature, $[\alpha]_{300}$ increases sharply at $T \sim 50$°C, confirming the sigmoidal increases found by previous authors, while b_0 decreases sigmoidally and levels off at a value fairly close to zero above 70°C. Thus, we find that although the $[\alpha]_{300}$ value in the aqueous salt at 70°C and that in pure cadoxen at 25°C are quite different (see Fig. 2), b_0 in these solvents are nearly equal. This demonstrates that b_0 for xanthan is far less sensitive to solvent conditions than $[\alpha]_{300}$. However, nothing can be deduced from b_0 data as to whether disordered xanthan in 0·01 M aqueous NaCl at 70°C is dispersed as completely separated chains.

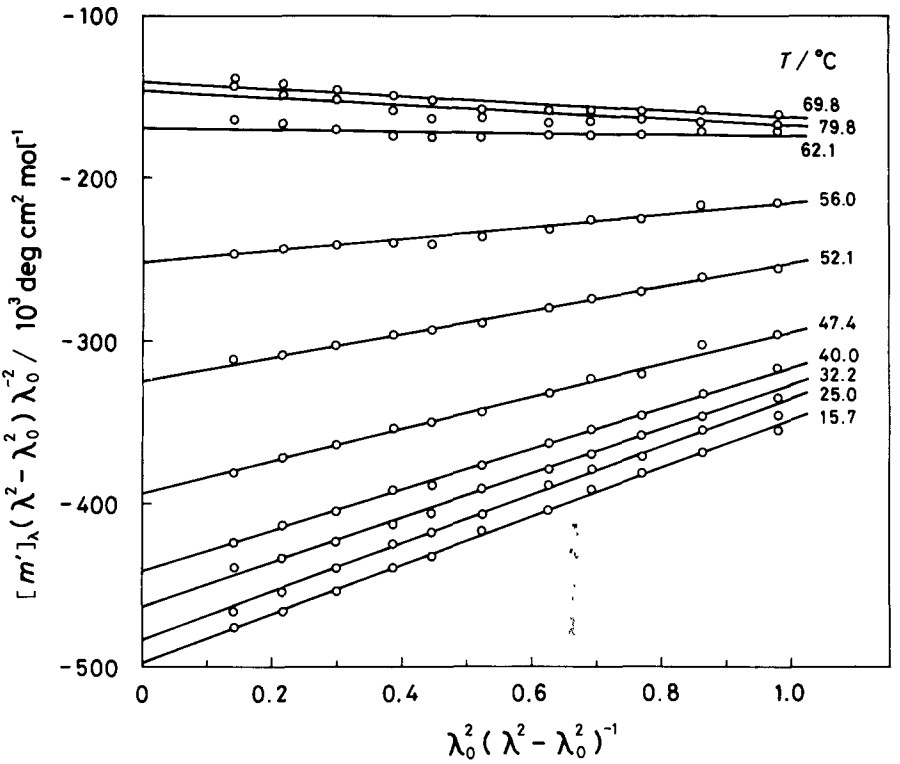

Fig. 7. Moffitt plots for sample X9-3 in 0·01 M aqueous NaCl at different temperatures ($c = 0{\cdot}498 \times 10^{-2}$ g cm^{-3} at 25°C).

The filled circles in Fig. 8 represent the values of $[\alpha]_{300}$ and b_0 for the xanthan double helix in 0·1 M aqueous NaCl. As expected, this b_0 value agrees with those in 0·01 M aqueous NaCl below 30°C (about 150×10^3 deg cm^2 mol^{-1}), which, however, are far below the b_0 value of 207×10^3 deg cm^2 mol^{-1} for the double helix in CMW. This discrepancy shows the limitations of the Moffitt parameter when applied to xanthan solutions.

Though not shown here, there exists an approximately linear relation between the $[\alpha]_{300}$ and b_0 data in Fig. 8. This implies that these optical parameters are essentially equivalent for 0·01 M aqueous NaCl solutions of xanthan in the temperature range studied in this work.

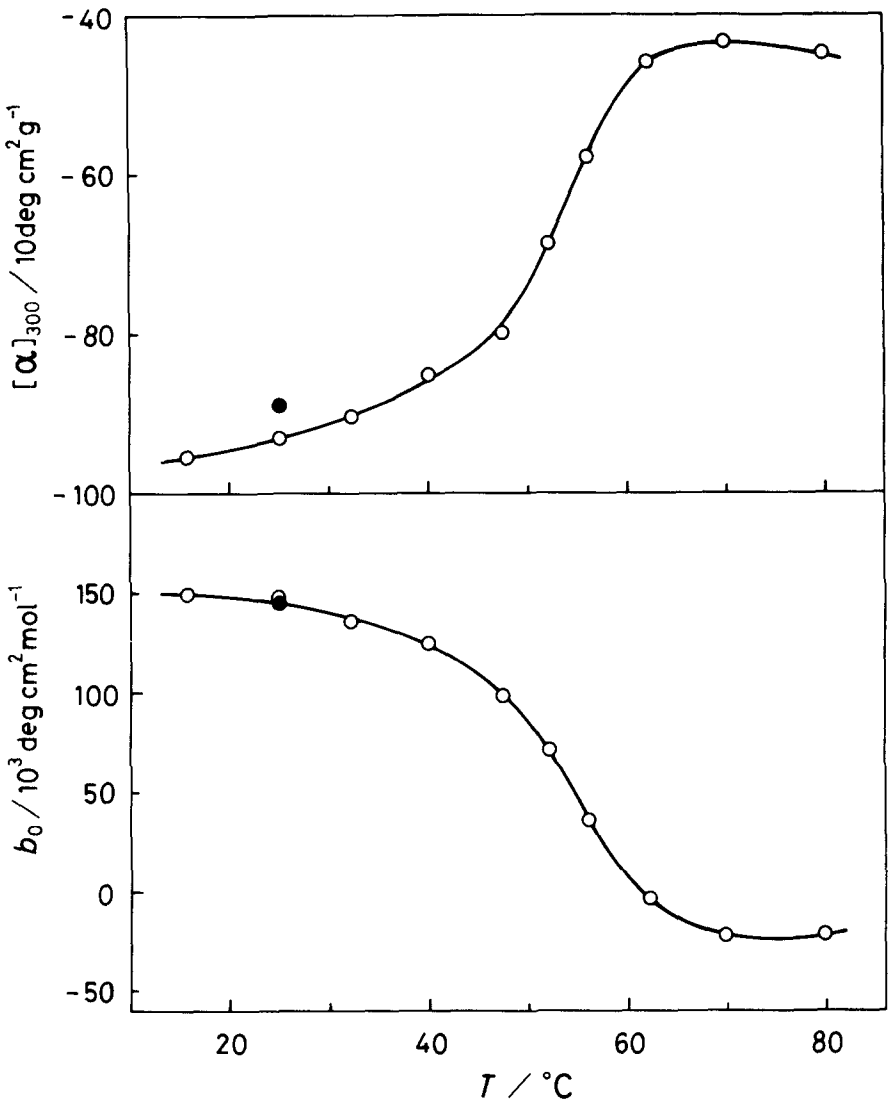

Fig. 8. Temperature dependence of $[\alpha]_{300}$ and b_0 for sample X9-3 in 0·01 M aqueous NaCl. ●, data in 0·1 M aqueous NaCl at 25°C.

ACKNOWLEDGEMENTS

This work was supported in part by the Institute of Polymer Research, Osaka University. We thank Professor A. Teramoto for his advice and valuable comments on the manuscript.

REFERENCES

Frangou, S. A., Morris, E. R., Rees, D. A., Richardson, R. K. & Ross-Murphy, S. B. (1982). *J. Polym. Sci., Polym. Lett. Ed.* **20**, 531.

Holzwarth, G. (1976). *Biochemistry* **15**, 4333.

Milas, M. & Rinaudo, M. (1979). *Carbohydr. Res.* **76**, 189.

Milas, M. & Rinaudo, M. (1981). In: *Solution Properties of Polysaccharides*, ed. D. A. Brant, ACS Symp. Ser., No. 150, Am. Chem. Soc., Washington, DC, p. 25.

Moffitt, W. & Wang, J. T. (1956). *Proc. Natl. Acad. Sci., US* **42**, 596.

Morris, E. R., Rees, D. A., Young, G., Walkinshaw, M. D. & Darke, A. (1977). *J. Mol. Biol.* **110**, 1.

Norton, I. T., Goodall, D. M., Morris, E. R. & Rees, D. A. (1980). *J. Chem. Soc., Chem. Commun.* 545.

Norton, I. T., Goodall, D. M., Frangou, S. A., Morris, E. R. & Rees, D. A. (1984). *J. Mol. Biol.* **175**, 371.

Okuyama, K., Arnott, S., Moorhouse, R., Walkinshaw, M. D., Atkins, E. D. T. & Wolf-Ullish, Ch. (1980). *Fiber Diffraction Methods*, eds A. D. French and K. H. Gardner, ACS Symp. Ser., No. 141, A.n. Chem. Soc., Washington, DC, p. 411.

Rees, D. A. (1981). *Pure Appl. Chem.* **53**, 1.

Sato, T., Norisuye, T. & Fujita, H. (1984*a*). *Polym. J.* **16**, 341.

Sato, T., Kojima, S., Norisuye, T. & Fujita, H. (1984*b*). *Polym. J.* **16**, 423.

Sato, T., Norisuye, T. & Fujita, H. (1984*c*). *Macromolecules* **17**, 2696.

Sato, T., Norisuye, T. & Fujita, H. (1985). *Polym. J.* **17**, 729.

Teramoto, A. & Fujita, H. (1976). *J. Macromol. Sci.-Rev. Macromol. Chem.* **C15**, 165.

Urnes, P. & Doty, P. (1961). *Adv. Protein Chem.* **16**, 401.